

<sup>1</sup>*The Fermi Surface*, edited by W. A. Harrison and M. R. Webb (Wiley, New York, 1961).

<sup>2</sup>R. Hartman, Phys. Rev. **181**, 1070 (1969).

<sup>3</sup>U. Hübner, Z. Naturforsch. **22**, 2086 (1967).

<sup>4</sup>H. J. Mackey and J. R. Sybert, Phys. Rev. **180**, 678 (1969).

<sup>5</sup>C. Herring and E. Vogt, Phys. Rev. **101**, 944 (1956).

<sup>6</sup>A. G. Samoylovich and I. I. Pinchuk, Phys. Metals Metallog. (USSR) (English transl.) **20**, 23 (1965).

<sup>7</sup>I. Ya. Korenblit, Fiz. Tverd. Tela **2**, 3083 (1960) [Soviet Phys. Solid State **2**, 2738 (1961)].

<sup>8</sup>A. H. Wilson, *The Theory of Metals*, (Cambridge U. P., Cambridge, England, 1958), p. 208 ff.

<sup>9</sup>H. Jones and C. Zener, Proc. Royal Soc. (London) **A145**, 268 (1934).

<sup>10</sup>Various ways of expanding  $[\hat{A}-\hat{B}]^{-1}$  are given in the Appendix of P. O. Löwdin, J. Math. Phys. **3**, 969 (1962).

<sup>11</sup>A. C. Smith, J. F. Janak, and R. B. Adler, *Electronic Conduction in Solids* (McGraw-Hill, New York, 1967).

<sup>12</sup>The  $\hat{\tau}$  of this paper is the transpose of the  $\hat{\tau}$  of Ref. 7 and Paper I, because in those papers the collision term is approximated as  $(\partial f_0/\partial \epsilon)\hat{\tau}^{-1}\hat{m}\hat{C}\cdot\hat{m}^{-1}\hat{p}$ .

<sup>13</sup>A. J. McConnell, *Applications of Tensor Analysis* (Dover, New York, 1957).

## New Method for Computing the Weak-Field Hall Coefficient. II. Some Extensions and Modifications\*

R. S. Allgaier

U. S. Naval Ordnance Laboratory, White Oak, Silver Spring, Maryland 20910

(Received 27 January 1970)

An earlier paper described a simple method for computing the weak-field Hall coefficient through the use of a Fermi surface composed entirely of planar faces. That paper developed a set of rules which linked the general behavior of the Hall coefficient to two fundamental properties of transport models, Fermi-surface shape and scattering anisotropy. The present paper reformulates those rules by adding a third ingredient to the model description, shape evolution. Exceptions to the earlier rules are thereby eliminated. The present paper also extends the simple method to noncubic models. The results for "undulating cylinders" (a Fermi-surface approximation for some hexagonal metals) and toroidal Fermi surfaces (a possible model for the wurtzite lattice) are analyzed. Finally, the effect of rounding the sharp edges at which the planar Fermi-surface faces intersect is investigated. The results resolve an apparent paradox pointed out by Stern, and provide some insight into the general magnetic field dependence of the Hall coefficient.

### I. INTRODUCTION

In an earlier paper, a new method was described for computing approximate values of the weak-field Hall coefficient  $R_0$ .<sup>1</sup> The essential feature of the procedure is to replace the actual Fermi surface by one composed entirely of planar faces. The advantage of the method is its simplicity; it is possible to obtain results for a wide variety of models, including those in which both Fermi-surface distortion and anisotropic scattering play an important role, without becoming involved in complicated mathematics.

The Hall coefficient ought to be one of the best understood transport coefficients; after all, it depends essentially on a single electronic parameter, charge density. But  $R_0$  is also influenced, in a more subtle way, by dimensionless functions of carrier velocity and scattering time. These functions stem from specific details of the model under consideration, but their effect on  $R_0$  has never been well understood in a broad sense.

Those few papers which do discuss the general

behavior of  $R_0$  generally relate it to two fundamental properties of a model, the shape of the Fermi surface and the scattering anisotropy. In I, we attempted to develop a set of rules for the behavior of  $R_0$  which were related to these two fundamental properties, and which would apply to all known models for which a scattering time was defined.

In Sec. II of the present paper, we reformulate those rules in terms of three fundamental model properties, the additional one being *shape evolution*, i. e., the manner in which the Fermi-surface shape changes as a function of the Fermi energy. As a consequence, we develop a distinctly different viewpoint from which to describe and understand the links between the essential characteristics of a model and the general behavior of  $R_0$ .

In I, all of the models discussed had over-all cubic symmetry. Section III of the present paper treats two noncubic models. Mathematically speaking, the extension is trivial and uninteresting. But the simple form of the results makes it possible to present, for the first time, a clear cut and realistic

explanation for the behavior of the two different Hall coefficients which occur in such noncubic systems.

Stern has pointed out that slightly rounding the edges between the planar faces of the Fermi surface can change the value of  $R_0$  substantially.<sup>2</sup> This paradoxical result is explained in Sec. IV. The study of the rounded-edge model also leads to other useful information.

The weak-field Hall coefficient may be written as

$$R_0 = r/ne, \quad (1)$$

where  $n$  is the carrier density,  $e$  is the charge on each carrier, and  $r$  is a dimensionless mixing factor. As discussed in I, it can be misleading to describe  $r$  as an anisotropy factor.

The viewpoint in the present paper focuses attention on the magnitude and sign of  $r$  which, it is to be emphasized, do not depend on the sign of the carriers. The normal sign of  $r$  is positive, corresponding to the situation in which the sign of the Hall coefficient and the sign of the carriers are the same.

In the present work, the models considered are treated in the metallic approximation. As shown in I, the method is easily extended to the case of classical statistics. Results for metals are particularly straightforward to calculate, however, since only simple algebra is required (there are no integrals to be evaluated).

## II. GENERAL BEHAVIOR OF $R_0$

The analysis in I led to the formulation of general rules which related the behavior of  $R_0$  to anisotropies of the Fermi surface and of the scattering time. For convenience, we reiterate those rules below. The Fermi surface was assumed to be entirely convex, and a scattering time  $\tau$  was assumed to exist.

(a) If  $\tau$  alone is anisotropic,  $r > 1$  for all models thus far investigated.

(b) If the Fermi surface alone is anisotropic,  $r < 1$  in *most* cases.

(c) If both types of anisotropy are present,  $r$  decreases or increases according to whether the  $\tau$  anisotropy emphasizes the flatter or sharper portions of the anisotropic Fermi surface. But as the  $\tau$  anisotropy becomes more and more extreme,  $r$  rises again, no matter which part of the surface is being emphasized. (In effect, some of the carriers disappear, so that the Hall coefficient grows larger.)

These rules were satisfying in their generality, but at that time we did not understand the circumstances which led to two exceptional cases, viz., those for which  $r > 1$  from shape anisotropy alone.

One exception is the Davis-Cooper-Raimes model<sup>3,4</sup> which will be discussed below in detail. In this case,  $r$  can become slightly greater than unity

$[(r-1) \ll 1]$  from a slightly distorted Fermi surface and isotropic  $\tau$ . A second exception is the cubically symmetric multivalley version of the Cohen model.<sup>5</sup> In this case, the energy-momentum relation in each valley is nonparabolic and nonellipsoidal, but  $\tau$  is isotropic. For certain ranges of the model parameters,  $r$  becomes as large as 1.2, and the behavior of  $r$  as a function of the model parameters suggests that still higher values are possible.

Trying to understand the behavior of  $r$  for these exceptional cases has led us to recognize that the traditional description of a transport model in terms of shape and  $\tau$  anisotropies is incomplete. A third fundamental characteristic must be added, shape evolution, i. e., the manner in which the shape of the Fermi surface changes as a function of energy. The revised description then goes as follows:

First of all,  $r$  should be regarded as a consequence of the Fermi-surface shape when no shape evolution and no  $\tau$  anisotropy are present. This basic value of  $r$  will then be altered by *two weighting factors*, shape evolution and  $\tau$  anisotropy.

The above description constitutes a distinctly different point of view from that found in I and in earlier discussions. Davis,<sup>3</sup> for example, talked about the "one-way equivalence" of Fermi-surface distortion and  $\tau$  anisotropy, i. e., any given value of  $r$  due to  $\tau$  anisotropy alone can be reproduced by an equivalent Fermi-surface distortion, but not *vice versa*. Our present approach places the Fermi-surface shape on a pedestal by itself; the equivalence principle is only applied between shape evolution and scattering anisotropy.

As will be shown below, the revised model description eliminates the exceptional cases. But it was not chosen simply because it has this useful consequence. It follows rather from an examination of the nature of the integrals which constitute the conventional Jones-Zener solution to the Boltzmann equation.<sup>6</sup>

For the metallic case, there are Fermi-surface curvature terms which ultimately determine the enclosed volume, i. e., the carrier density. Mixed up with these are dimensionless functions of the Fermi velocity  $v_F$  and of  $\tau$ , i. e., functions of the relative values of each parameter on different parts of the Fermi surface.

But if there is no shape evolution, then the relative values of  $v_F$  are fixed by the Fermi-surface shape. And if there is no  $\tau$  anisotropy,  $\tau$  cancels from the integrals, and  $r$  is determined by the Fermi-surface shape alone.

In terms of this new description, the rules for the general behavior of  $r$  become:

(a) For all distorted Fermi surfaces,  $|r| < 1$ , provided that the shape does not change with energy and that  $\tau$  is isotropic. (Introducing the absolute

value sign allows the above to include surfaces which are convex, concave, or a combination of both types of curvature.)

(b) For a spherical convex or concave Fermi surface,  $|r| > 1$  whenever either or both of the two weighting factors, shape evolution or scattering, introduce anisotropies.

(c) For a distorted Fermi surface which is either entirely convex or entirely concave,  $|r|$  decreases or increases according to whether the weighting factors, acting singly or in combination, emphasize the flatter or sharper portions of the Fermi surface. But when the weighting becomes too anisotropic,  $|r|$  rises again. For a surface which has both convex and concave portions, there is the additional possibility that  $r$  will change sign before its magnitude begins to increase again.

It is to be emphasized that the above rules do not have mathematical proofs to back them up. But so far as we know they are consistent with every Hall-coefficient calculation that has ever been carried out for a single-band model (including multivalley models) which assumes the existence of a scattering time.

We may now reinterpret the behavior of  $r$  found in the Davis-Cooper-Raimes model.<sup>3,4</sup> Their investigations were important because they led to a simple expression for  $r$  which allowed the effects of shape and  $\tau$  anisotropies to be assessed separately or in combination. The result is

$$1/r = 1 + \frac{4}{21} [9A^2 + 18A(B - C) - (B - C)^2], \quad (2)$$

where the parameters  $A$ ,  $B$ , and  $C$  are restricted to values much smaller than unity.

As we mentioned earlier, Davis observed that when the Fermi surface is spherical ( $A = B = 0$ ) and  $\tau$  is anisotropic ( $C \neq 0$ ),  $r > 1$ , always. But when  $\tau$  is isotropic ( $C = 0$ ) but the Fermi surface is not ( $A, B \neq 0$ ),  $r$  may be greater than or less than unity. The implication has been that  $r$  will increase or decrease according to the *type* of Fermi-surface distortion present; e.g., will the surface bulge or be depressed in the  $\langle 111 \rangle$  directions of momentum space?

A closer look at the significance of the parameters of Eq. (2) reveals that  $A$  specifies the shape and  $B$  the shape evolution of the Fermi surface. When  $B = A$  the shape (distorted or not) does not change with energy. Under these conditions,  $1/r = 1 + \frac{104}{21} A^2$  when  $C = 0$ ; i.e., when  $\tau$  is isotropic, a distorted Fermi surface of unchanging shape *always* makes  $r < 1$ .

It is also clear from Eq. (2) that the effects of shape evolution and  $\tau$  anisotropy are equivalent; the condition is  $C = -B$ . Furthermore, for a spherical Fermi surface which is not spherical at other energies ( $A = 0$ ,  $B \neq 0$ ),  $1/r = 1 - \frac{4}{21} (B - C)^2$ , so that anisotropic scattering, or an evolving shape,

or both, always make  $r > 1$ . (In this simple model, the two effects can exactly cancel each other when  $C = B$ .)

Thus the Davis-Cooper-Raimes model conforms to the revised rules in all respects.

The other exception under the old rules was the cubically symmetric version of the Cohen model.<sup>5</sup> In that study, an anisotropic  $\tau$  was not considered, and the Fermi-surface shape always changed with energy. To show that  $r$  does not exceed unity when the shape does not evolve would require an entirely new and very tedious calculation.

One circumstance under which  $r > 1$  in the Cohen model is obviously consistent with the revised rules. It is the case when  $\mu = 0$  ( $\mu$  is the interband mass ratio in the model). Then the Fermi surface remains ellipsoidal at all energies, but it becomes less prolate and ultimately oblate as the energy increases. At the energy for which the surface is spherical,  $r > 1$ , in accord with revised rule (b).

The other circumstance under which  $r > 1$  in the cubically symmetric Cohen model occurs when the Fermi surface acquires a very highly distorted dumbbell shape which is changing very rapidly with energy. It seems obvious that shape evolution plays a dominant role in this case, but at present we cannot say anything more specific about this very extreme situation.

### III. EXTENSION TO NONCUBIC MODELS

Most of the models investigated in I were highly anisotropic, but they all had over-all cubic symmetry. Consequently, there was only one Hall coefficient. For a noncubic model, the expression analogous to Eq. (2) of I is

$$R_0 = E(-i_{yx})/i_x i_y H. \quad (3)$$

The currents  $i_x$  and  $i_y$  are those which result when the electric field  $E$  is applied in the positive  $x$  and  $y$  directions, with the magnetic field  $H = 0$ . The Hall current  $i_{yx}$  results when  $E$  and  $H$  are in the positive  $x$  and  $z$  directions, respectively. (In I,  $i_{yx}$  was simply called  $i_y$ , since  $E$  was always applied in the  $x$  direction only.) It is important to note that the Hall current is due entirely to those carriers which drift across an edge of the Fermi surface, i.e., pass from one planar face to an adjacent one.

There are two Hall coefficients for crystals with hexagonal symmetry. In such materials, the experimental value of the Hall coefficients with  $H$  parallel to the symmetry axis  $R_0(\parallel)$  is usually "well behaved," i.e.,  $r \approx +1$ . When  $H$  is perpendicular to the symmetry axis, however, the Hall coefficient  $R_0(\perp)$  is often much smaller, may be negative or positive, and may depend strongly on temperature.<sup>7</sup>

It is possible to describe the temperature dependence of  $R_0(\perp)$  with a simple, isotropic, two-band

model having electrons in one band and holes in the other, by assigning the proper temperature dependence to the carrier mobilities. Such a model will of course allow either sign for  $r$ . This kind of model was used by Lee and Legvold to discuss the behavior of  $R_0(\perp)$  in lutetium and yttrium.<sup>8</sup> But the model is isotropic, and cannot at the same time describe the behavior of the much larger and nearly temperature independent  $R_0(\parallel)$ . Hence it does not provide any information about the essential features of the real band model.

A more realistic basis for analyzing the Hall-coefficient behavior in hexagonal metals is provided by the planar-faced model shown in Fig. 1. This model has tetragonal symmetry, but as far as the Hall-coefficient behavior is concerned, there is no distinction between hexagonal and tetragonal symmetry. The latter was used because it is particularly straightforward to calculate  $r$  when the planar faces are orthogonal to one another.

The Fermi surface in Fig. 1 may be regarded as an approximation to a right-circular "cylinder" with an undulating cross section. The surface is, of course, endless; the dotted lines in the figure indicate its intersection with the ends of the Brillouin zone. With  $H$  parallel to the symmetry axis, all carriers move on the Fermi surface in planes perpendicular to the axis; this corresponds to the well-

behaved component  $R_0(\parallel)$ . When  $H$  is perpendicular to the symmetry axis, the carriers drift along the Fermi surface, parallel to its axis, and hence some of them turn to the right and some to the left.

As shown in Fig. 1, the size and shape of the Fermi surface are specified  $p_t$  and  $p_t'$ , and by  $p_t'$  and  $p_t'$ , for the thicker and thinner portions of the Fermi surface. Three Fermi velocities are also identified,  $v_t$  and  $v_t'$  for the thicker, and  $v_t'$  for the thinner part of the surface. We wish to consider the simplest possible model which can account qualitatively for the experimental data, and therefore it will be assumed that the scattering time  $\tau$  is constant over the entire Fermi surface.

We compute  $i_x$ ,  $i_y$ , and  $i_{yx}$  for the two configurations, using the axes specified in Fig. 1. For  $H$  parallel to the symmetry axis,

$$i_x = i_y = (4/h^3) [(4p_t p_t') (eE\tau) (ev_t) + (4p_t' p_t') (eE\tau) (ev_t')] , \quad (4)$$

$$i_{yx} = (4/h^3) [(2p_t) (eE\tau) (ev_t H\tau) (ev_t) + (2p_t') (eE\tau) (ev_t' H\tau) (ev_t')] , \quad (5)$$

and

$$n = (2/h^3) (8p_t^2 p_t + 8p_t'^2 p_t') . \quad (6)$$

Substituting these three equations into Eq. (3) reveals that the result may be expressed in a more compact form by defining the following dimensionless ratios:  $K = p_t/p_t'$ ,  $L = p_t'/p_t'$ ,  $f = p_t'/p_t$ , and  $1/f' = v_t'/v_t$ .

The result becomes

$$R_0(\parallel) = \frac{1}{2ne} \frac{(f'^2 K + fL)(K + f^3 L)}{(f'K + f^2 L)^2} . \quad (7)$$

Clearly, the above may be written as a function of the ratio  $K/L$  only. Thus the answer depends only on the relative volumes of the thicker and thinner portions of the Fermi surface (determined by  $f$  and  $K/L$ ), on the relative shapes of the two parts ( $K/L$ ), and by the relative values of the transverse Fermi velocities ( $f'$ ). The same remarks hold for the other component of  $R_0$ , which is

$$R_0(\perp) = \frac{1}{2ne} \frac{(f' - f)(K + f^3 L)}{(1 - f^2)(f'K + f^2 L)} . \quad (8)$$

The definitions for  $f'$  and  $f$  were chosen such that  $f' = f$  (i. e.,  $v_t' p_t' = v_t p_t$ ) corresponds to the condition that the shape of the Fermi surface does not change with energy. Equation (8) shows that  $R_0(\perp) = 0$  under this condition, and has opposite signs for  $f' > f$  and  $f' < f$ .

According to this model, the relatively small size and temperature sensitivity of  $R_0(\perp)$  seen experimentally imply that the effects of the concave and convex portions of the Fermi surface nearly cancel each other. A wide range of parameters correspond to this near cancellation while at the same time pre-

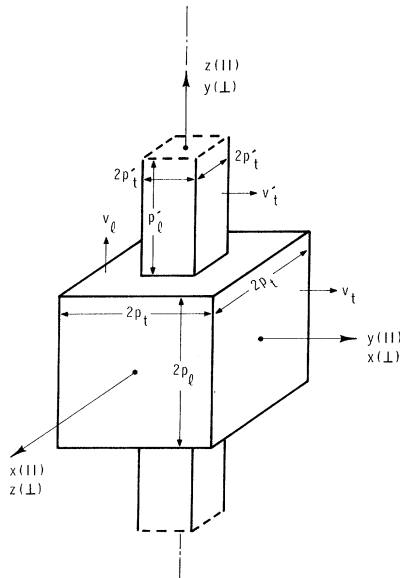


FIG. 1. A tetragonal planar-faced approximation to the Fermi surface of some hexagonal metals. The symbols  $\parallel$  and  $\perp$  following  $x$ ,  $y$ , and  $z$  identify the axes for computing the Hall-coefficient components when the magnetic field is parallel to and perpendicular to the symmetry axis, respectively. The symbols  $p$  and  $v$  identify various dimensions of the Fermi surface (in momentum space) and Fermi velocities on the nonequivalent faces, respectively.

dicting a normal magnitude for  $R_0(\parallel)$ .

For example, let  $K=1$ ,  $L=3$ , and  $f=\frac{1}{3}$ ; then the thicker part of the Fermi surface is a cube, and the thinner part has the same length as the thicker part, but only  $\frac{1}{3}$  the width. Furthermore, let  $f'=\frac{1}{2}$ ; this means that the neck is filling in as the Fermi surface grows. Consequently, the Fermi velocity on the neck is decreased and the importance of the convex portion of the Fermi surface is enhanced. Thus,  $R_0(\perp)$  should have the normal sign, which it does.

The results for the above case are  $R_0(\parallel) = 1/ne$  and  $R_0(\perp) = \frac{1}{8}/ne$ . This may be described as typical of the kind of experimental Hall data found in hexagonal metals. In accordance with the discussion in Sec. II, the same results could have been obtained for the above model if no shape evolution were allowed, but instead the scattering times on the transverse faces of the thicker and thinner parts of the Fermi surface were assumed to differ from each other.

A planar-faced Fermi surface is also useful for discussing the behavior of  $R_0$  for the case of toroidal energy surfaces. Such a surface is possible in crystals having the wurtzite lattice.<sup>9</sup> Again, a model with tetragonal symmetry is equivalent to the symmetry of the actual Fermi surface, as far as the behavior of  $R_0$  is concerned.

The model and the pertinent parameters are shown in Fig. 2(a). The scattering time is assumed to be the same on all faces. In this case, the "normal" component occurs when  $H$  is perpendicular to the axis of the "torus." The result is

$$R_0(\perp) = \frac{1}{2}/ne \quad (9)$$

(the same as for a simple cube), regardless of the values of the six parameters of the model.

If we define the ratios  $f_p = p_i/p_0$  and  $f_v = v_i/v_0$ , the result for the "anomalous" component is

$$R_0(\parallel) = \frac{1}{2ne} \frac{(1-f_v^2)(1-f_p^2)}{(1+f_v f_p)^2} \quad (10)$$

At first glance, this seems to be a strange and perhaps nonsensical result. It predicts, for instance, that when  $v_i = v_0$ , then  $R_0(\parallel) = 0$ , no matter how small the hole in the torus becomes.

But Fig. 2(b) suggests a more realistic velocity profile for use with Eq. (9). It indicates that  $v_i \ll v_0$  ( $f_v \approx 0$ ) when the hole is small ( $f_p \approx 0$ ). Hence a small hole brings about only a slight deviation (towards smaller values) from the holeless result ( $\frac{1}{2}/ne$ ). As the hole grows,  $neR_0(\parallel)$  steadily decreases, corresponding to the growth of the opposing contribution from countercirculating electrons on the inner surface. For the velocity profile shown in Fig. 2(b), however,  $v_i$  is always less than  $v_0$ , so that  $neR_0(\parallel)$  approaches zero as  $p_i \rightarrow p_0$  without changing sign.

#### IV. ROUNDING THE EDGES OF A PLANAR-FACED FERMI SURFACE

When the scattering time  $\tau$  is assumed to be isotropic, the mixing factor  $r$  becomes identical with a quantity  $\mathcal{R}$  which can be obtained from Faraday-effect measurements.<sup>10</sup> Stern has shown that  $\mathcal{R}$  can be written in terms of an integral over the Fermi surface containing the reciprocals of the two principal radii of curvature of the Fermi surface at each point.<sup>11</sup>

The factor  $\mathcal{R}$  is easily evaluated for the case of a cube. To avoid infinities in the integral mentioned above, it is necessary to "slightly round" the edges of the cube, i.e., give them a small but finite radius of curvature. The result is<sup>2</sup>

$$\mathcal{R} = \frac{1}{4}\pi = 0.785 \quad (11)$$

This is about 50% larger than the value  $r = \frac{1}{2}$  [Eq. (6) of I] which was obtained for the cube.

The two models used appear to be very nearly the same, so that the large difference between the results is very puzzling. It turns out that the assumptions regarding the magnitude of  $H$  were such that the models do become quite different.

Because of the sharp edges of the planar-faced Fermi surface used to calculate  $r$ , all carriers either do or do not go around an edge of the surface; none go "part way around an edge." In determining  $\mathcal{R}$ , on the other hand, carriers on the slightly curved edges of the Fermi surface were assumed to turn through a very small angle during the time  $\tau$ . Thus  $\mathcal{R}$  was calculated under magnetic field conditions such that the Hall angles for *all* carriers are small. This condition is unattainable for the Fermi surface with sharp edges; for a small enough  $H$ , the

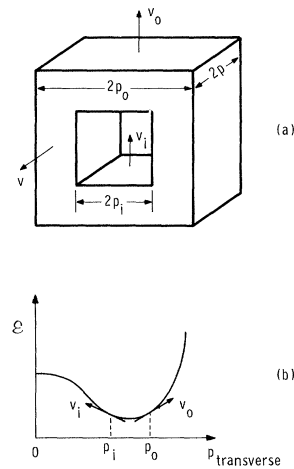


FIG. 2. (a) A planar-faced approximation to a toroidal Fermi surface. The symbols  $p$  and  $v$  identify Fermi-surface dimensions and Fermi velocities, respectively. (b) An energy-momentum curve from which reasonable values of  $v_i$  and  $v_0$  can be estimated for the model in (a).

average value of the Hall angle will become small, but it can never be small for those carriers which go around a corner.

Nevertheless, it remains appropriate to regard a sharp-edged Fermi surface as an approximation to one which has finite radii of curvature everywhere. However, the values of  $r$  calculated with this point of view in mind more properly correspond to a "mixed-field" situation for the real model, i. e., the magnitude of  $H$  is such that it lies in the weak-field range for some carriers, but in the strong-field range for others.

If the ultimate, weak-field-for-all-carriers limit of  $r$  is desired, it is obtainable with very little additional calculation. This is shown in the Appendix for the case of the slightly rounded cube. It gives  $r = \frac{1}{4}\pi$ , as it should.

If a Fermi surface can be divided into well-defined areas which are relatively sharp and relatively flat,<sup>12</sup> then over some intermediate range of  $H$  a "mixed-field" value of  $r$  should occur which differs from both the weak-field and strong-field limits. If such an intermediate-field plateau were found experimentally, it could be used to determine  $\tau$  on the sharp portions of the Fermi surface if the shape of the Fermi surface were well known, or vice versa.

## V. CONCLUDING REMARKS

With the aid of computers, numerical values of the weak-field Hall coefficient may be accurately determined for very complicated models. And it has become clear that almost all realistic band models for crystals do have complicated shapes when the Fermi level is not very close to a band edge. However, calculating precise results for a particular model does not add much to the understanding of the Hall coefficient unless it illuminates the connection between what went into the calculation and what came out.

The first attempt (in I) to discuss the connections between the general behavior of  $r$  and the basic ingredients of the models used for the calculation was defective in that it did not recognize the importance of the shape-evolution factor. We believe that Sec. II of the present paper does contain a complete discussion of those connections.

We also wanted to demonstrate some useful applications of the mathematically trivial extension of the method to noncubic models. And finally, we wanted to make it clear why a slight rounding of the edges between the planar faces of the Fermi surface can have such a significant effect on the magnitude of  $r$ .

In conclusion, we again note, as we had in I, that a Fermi surface with planar faces *and* sharp edges cannot be used to calculate a true weak-field magnetoresistance. But the calculation does become possible if the edges are slightly rounded. The

mathematics is a little more involved than in the case of the Hall coefficient, but not nearly as complicated as other magnetoresistance calculations involving anisotropic nonellipsoidal Fermi surfaces. This extension to weak-field magnetoresistance will be presented in a separate paper.

## ACKNOWLEDGMENT

I am indebted to E. A. Stern for pointing out the connection between  $r$  and  $\mathcal{R}$ , and for carrying out a calculation of  $\mathcal{R}$ , using his method, for a cube with slightly rounded edges.

## APPENDIX: CALCULATION OF $r$ FOR A SLIGHTLY ROUNDED CUBE

The calculation follows the procedure described in Sec. III. "Slightly rounded" implies that the curved portions of the Fermi surface constitute a very small fraction of the total surface area and introduce a negligible change in the total carrier density enclosed by the Fermi surface. Hence, the results for  $i_x$ ,  $i_y$ , and  $n$  are the same as for the sharp-edged cube [Eqs. (3) and (5) of I],

$$i_x = i_y = (4/h^3)(8p^2 e E \tau)(ev), \quad (\text{A1})$$

where the separation of opposite flat faces of the surface is  $2p$ ,  $v$  is the Fermi velocity on the flat portions of the Fermi surface, and

$$n = (2/h^3)(2p)^3. \quad (\text{A2})$$

The Hall current  $i_{yx}$  may be computed with the aid of Fig. 3. We assume that the Fermi velocity on the rounded edges of the surface is the same as on the flat faces. It is also assumed that  $H$  is so small

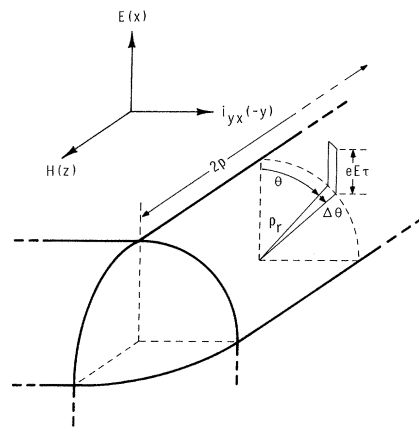


FIG. 3. Pictorial description of the calculation of the Hall current for a slightly rounded cube-shaped Fermi surface. The coordinate axes identify the directions of the applied fields  $E$  and  $H$  and the resulting Hall current  $i_{yx}$ . In momentum space, the forces displace the carriers by the distances  $eE\tau$  and  $p_r \cos \theta \Delta \theta$  in the  $p_x$  and  $p_y$  directions, respectively, where  $p_r$  is the radius of curvature of the rounded edge of the Fermi surface and  $\Delta \theta$  is the angle through which the Fermi velocity turns in the time  $\tau$ .

that carriers on these curved surfaces turn through a small angle  $\Delta\theta$  in the time  $\tau$ ; consequently, contributions from carriers which cross the boundaries between the flat and curved regions Fermi surface may be neglected. The contributions from the rounded *corners* may also be neglected. The only contribution to the Hall current which needs to be considered is

$$i_{yx} = \left(\frac{4}{h^3}\right) \int_{-\pi/2}^{\pi/2} \{[(2p)(eE\tau)(p_r \cos \theta d\theta)]$$

$$\times e[v \sin(\theta + \Delta\theta) - v \sin \theta]\} , \quad (A3)$$

where  $p_r$  is the radius of the curved cylindrical surface and  $\Delta\theta = evH\tau/p_r$ . The three momentum factors in the first square bracket determine the differential volume element of contributing carriers and the second bracket gives the change in their transverse velocity.

The numerical coefficient of Eq. (A3), after integration, is  $4\pi$  instead of the 8 which was obtained for the sharp-edged cubic [see Eq. (4) of I]. Hence,  $r = \frac{1}{4}\pi$  rather than  $\frac{1}{2}$ .

\*Work supported in part by ONR Contract No. PO-9-0163.

<sup>1</sup>R. S. Allgaier, Phys. Rev. **165**, 775 (1968), hereafter referred to as I.

<sup>2</sup>E. A. Stern (private communication).

<sup>3</sup>L. Davis, Phys. Rev. **56**, 93 (1939).

<sup>4</sup>J. R. A. Cooper and S. Raimes, Phil. Mag. **4**, 145 (1959).

<sup>5</sup>R. S. Allgaier, Phys. Rev. **152**, 808 (1966).

<sup>6</sup>H. Jones and C. Zener, Proc. Roy. Soc. (London) **A145**, 268 (1934).

<sup>7</sup>As, for example, in Zn and Cd: see Landolt-Börnstein, *Zahlenwerte und Funktionen* (Springer-Verlag,

Berlin, 1959), 6th ed., Vol. 2, Part 6, p. 169.

<sup>8</sup>R. S. Lee and S. Legvold, Phys. Rev. **162**, 431 (1967).

<sup>9</sup>A. G. Aronov and P. Kh. Musaev, Fiz. Tverd. Tela **9**, 2284 (1967) [Soviet Phys. Solid State **9**, 1790 (1968)].

<sup>10</sup>E. A. Stern, *Optical Properties and Electronic Structure of Metals and Alloys* (North-Holland, Amsterdam, 1966), p. 599.

<sup>11</sup>E. A. Stern, Bull. Am. Phys. Soc. **5**, 150 (1960); Univ. of Maryland Tech. Report No. 261 (unpublished).

<sup>12</sup>For example, the second band of Al [W. A. Harrison, Phys. Rev. **118**, 1190 (1960)] and the hole octahedron of W [L. F. Mattheiss, *ibid.* **139**, A1893 (1965)].

## de Haas-van Alphen Effect in Thallium<sup>†</sup>

Y. Ishizawa\* and W. R. Datars<sup>‡</sup>

*Department of Physics, McMaster University, Hamilton, Ontario, Canada*

(Received 13 July 1970)

The de Haas-van Alphen (dHvA) effect in single crystals of high-purity thallium has been investigated in magnetic fields up to 55 kOe. These measurements extend previous work by providing accurate dHvA frequencies for field directions in the three principal crystallographic planes. dHvA frequencies larger than  $10^7$  G are assigned to orbits on the third-zone hole surface centered at *A* and the fourth-zone hexagonal network of Soven's relativistic orthogonalized-plane-wave model. Comparisons with the single-orthogonalized-plane-wave Fermi-surface model are also made. Magnetic breakdown of some of the orbits is observed. Lower dHvA frequencies are assigned to a small dumbbell-shaped surface with symmetry  $\bar{6}m2$ . The cyclotron masses of orbits on this surface are also presented and compared with recent cyclotron resonance results.

### I. INTRODUCTION

There have been recent investigations of the Fermi surface of thallium using magnetoresistance,<sup>1-5</sup> the magnetoacoustic effect,<sup>6-8</sup> cyclotron resonance,<sup>9,10</sup> and the de Haas-van Alphen (dHvA) effect.<sup>11-16</sup> The dHvA frequency is proportional to the extremal cross-sectional area of the Fermi surface normal to the magnetic field direction. It is therefore important to have complete accurate dHvA measurements as a function of magnetic field direction. They are useful for determining features

of the Fermi surface and for deriving the band structure and Fermi surface by the pseudopotential method.

Some high dHvA frequencies were measured by Priestley using pulsed magnetic fields<sup>13</sup> and will be compared with the present results wherever possible. Low dHvA frequencies were observed by the present authors,<sup>14</sup> Anderson, Schirber, and Stone,<sup>15</sup> and Saito.<sup>12</sup> These low-frequency results were extended by Capocci *et al.*<sup>16</sup> and interpreted in terms of a small dumbbell-shaped Fermi surface